

Absorption of light by extremely shallow metallic gratings: metamaterial behavior

Evgeny Popov, Stefan Enoch, and Nicolas Bonod

Institut Fresnel, Aix-Marseille Université, CNRS, Faculté St-Jérôme, 13397 Marseille Cedex 20, France
e.popov@fresnel.fr

Abstract: Extremely shallow lamellar metallic gratings are shown to totally absorb incident light inside a wide angular interval. The full absorption still holds at the homogenization limit when the period tends toward zero. It is shown that a lamellar grating, illuminated in normal incidence and in transverse magnetic polarization with a period lower than $1/\lambda$, of the vacuum wavelength behaves like a dielectric one with a high refractive index. The full absorption is then not due to the excitation of surface plasmon but either to Fabry-Perot resonance or Brewster effect, depending on the corrugated layer thickness.

©2009 Optical Society of America

OCIS codes: (050.0050) Diffraction and gratings; (240.0240) Optics at surfaces; (240.6680) Surface plasmons

References and links

1. R. W. Wood, "On a remarkable case of uneven distribution of light in a diffraction grating spectrum," *Philos. Mag.* **4**, 396-402 (1902)
2. U. Fano, "The theory of anomalous diffraction gratings and of quasi-stationary waves on metallic surfaces (Sommerfeld's waves)," *J. Opt. Soc. Am.* **31**, 213-222 (1941)
3. D. A. Weitz, T. J. Gramila, A. Z. Genack, and J. I. Gersten, "Anomalous low-frequency Raman scattering from rough metal surfaces and the origin of the surface-enhanced Raman scattering," *Phys. Rev. Lett.* **45**, 355-358 (1980).
4. R. Reinisch and M. Nevière, "Electromagnetic theory of diffraction in nonlinear optics and surface-enhanced nonlinear optical effects," *Phys. Rev. B* **28**, 1870-1885 (1983)
5. W. L. Barnes, A. Dereux, T. W. Ebbesen, "Surface plasmon subwavelength optics," *Nature* **424**, 824-829 (2003)
6. M. C. Hutley and D. Maestre, "Total absorption of light by a diffraction grating," *Opt. Commun.* **19**, 431-436 (1976)
7. M. Nevière, D. Maestre, R. C. McPhedran, G.H. Derrick and M.C. Hutley, "On the total absorption of unpolarized monochromatic light," *Proceedings of the ICO-11 Conference, Madrid, Spain*, pp. 609-612 (1978)
8. E. Popov, D. Maestre, R.C. McPhedran, M. Nevière, M.C. Hutley, and G. H. Derrick, "Total absorption of unpolarized light by crossed gratings," *Opt. Express* **16**, 6146-6155 (2008)
9. E. Popov, S. Enoch, G. Tayeb, M. Nevière, B. Gralak, N. Bonod, "Enhanced transmission due to non-plasmon resonances in one and two dimensional gratings," *Appl. Opt.* **43**, 999-1008 (2004)
10. T. V. Teperik, F. J. García De Abajo, A. G. Borisov, M. Abdelsalam, P. N. Bartlett, Y. Sugawara, and J. J. Baumberg, "Omnidirectional absorption in nanostructured metal surfaces," *Nature Photon.* **2**, 299-301 (2008)
11. N. Bonod and E. Popov, "Total light absorption in a wide range of incidence by nanostructured metals without plasmons," *Opt. Lett.* **33**, 2398-2400 (2008)
12. P. M. Ajayan, "Experimental observation of an extremely dark material made by a low-density nanotube array," *Nano. Lett.* **8**, 446 (2008)
13. V. G. Kravets, F. Schedin, A. N. Grigorenko, "Plasmonic blackbody: Almost complete absorption of light in nanostructured metallic coatings," *Phys. Rev. B* **78**, 205405 (2008).
14. J. Le Perchec, P. Quémenerais, A. Barbara, and T. López-Rios, "Why metallic surfaces with grooves a few nanometers deep and wide may strongly absorb visible light," *Phys. Rev. Lett.* **100**, 066408 (2008).
15. S. T. Peng, T. Tamir, and H. L. Bertoni, "Theory of periodic dielectric waveguides," *IEEE Trans. Microwave Theory and Techn.* **MTT-23**, 123-133 (1975).
16. E. I. Krupitsky and B. C. Chernov, "Rigorous analysis of arbitrary slanted volume holographic gratings," (in Russian), *Proc. IX All-Union School of Holography, Leningrad, 1977*, pp 84-95.

17. M. G. Moharam and T. K. Gaylord, "Rigorous coupled-wave analysis of dielectric surface-relief gratings," *J. Opt. Soc. Am.* **72**, 1385-1392 (1982).
 18. P. Lalanne and G. M. Morris, "Highly improved convergence of the coupled-wave method for TM polarization," *J. Opt. Soc. Am. A* **13**, 779-784 (1996).
 19. G. Granet and B. Guizal, "Efficient implementation of the coupled-wave method for metallic gratings in TM polarization," *J. Opt. Soc. Am. A* **13**, 1019-1023 (1996).
 20. L. Li, "Use of Fourier series in the analysis of discontinuous periodic structures," *J. Opt. Soc. Am. A* **13**, 1870-1876 (1996).
 21. M. Nevère and E. Popov, *Light Propagation in Periodic Media: Differential Theory and Design* (Marcel Dekker, New York, 2003).
 22. E. D. Palik, ed. *Handbook of Optical Constants of Solids* (Academic Press, 1985)
 23. <http://www.luxpop.com/>
 24. R. C. McPhedran, L. C. Botten, M. Craig, M. Nevière, and D. Maystre, "Lossy lamellar gratings in the quasistatic limit," *Opt. Acta* **29**, 289-312 (1982)
 25. G. Bouchitte and R. Petit, "Homogenization techniques as applied in the electromagnetic theory of gratings," *Electromagnetics* **5**, 17-36 (1985)
 26. E. Popov and S. Enoch, "Mystery of the double limit in homogenisation of finitely or perfectly conducting periodic structures," *Opt. Lett.* **32**, 3441-3443 (2007)
 27. J. C. Maxwell-Garnet, "Colors in metal glasses and in metallic films," *Philos. Trans. R. Soc. London Ser. A* **203**, 385-420 (1904)
 28. A. D. Yaghjian, "Electric dyadic *Green's* functions in the source region," *Proc. IEEE* **68**, 248-263, 1980
 29. M. Nevière, "The homogeneous problem," in *Electromagnetic theory of gratings*, R. Petit ed. (Springer-Verlag, 1980), Chap. 5
-

1. Introduction

Anomalous (unexpected) absorption of light by metallic diffraction gratings was observed at first by R. Wood [1], and it required half a century to explain this phenomenon by a resonant excitation of plasmon-polariton surface wave (PSW) that can propagate along the metal-air interface [2]. The grating periodicity enables the coupling between the PSW and the incident light, a fact that is of great importance in SERS [3], nonlinear optics [4], and recently in plasmonics [5]. About 30 years ago, Hutley and Maystre have predicted and observed total absorption of light by a shallow sinusoidal grating, with groove depth of the order of one tenth of wavelength [6]. As far as PSW can only propagate in transverse-magnetic (TM) polarization, a grating with one-dimensional periodicity is able to absorb only the half of unpolarized light, a disadvantage in solar cells optimisation and other unpolarized applications (optical telecommunications, luminescence spectroscopy, etc.). Two-dimensional periodicity (crossed gratings) can lead to strong unpolarized absorption [7, 8]. However, due to the sharply resonant nature of PSW excitation, the absorption is limited to small ranges of angles of incidence, rarely exceeding several degrees [6 - 8]. In order to increase the angular range, it is possible to use localized resonances, instead of unlocalized ones, for example cavity resonances [9]. Quite recently, an experimental realization of 2D array of dielectric spheres embedded below the metallic surface [10] has been shown to provide light absorption in unpolarized light in large angular interval, due to the excitation of cavity modes. Similar effect can be obtained without the help of plasmons using dielectric cylinders instead of spheres illuminated in transverse electric (TE) polarization [11]. Z. P. Yang et al. presented in 2008 an absorbing layer consisting of very thin aligned carbon nanotubes [12]. The optical device is based on a very low ratio between the diameter of the nanotubes (10 nm) and their spacing (50 nm), so that the real part of the effective refractive index of the device is close to one. The impinging light is not reflected and the small value of the imaginary part of the effective refractive index permits to absorb the incident light. The major drawback of this system is the requirement of a large thickness (300 μm). V. G. Kravets et al. proposed to reduce the thickness of the absorbing layer to a few hundred of nanometers by structuring periodically a gold layer [13]. The use of the Maxwell-Garnett effective theory permitted to show that the corrugated layer behaves like an homogeneous layer with a refractive index close to $1.6 + i 0.3$. A recent study has shown that very shallow lamellar gratings (10-15 nm deep, with wavelength λ around 450 nm) with period d about 30 nm can also lead to (almost)

total absorption of incident light [14], with a major advantage to propose an absorbing layer with a thickness between 10 or 15 nm.

The first aim of this paper is to show that it is possible to obtain light absorption with unpolarized light by using shallow lamellar metallic gratings with 2D periodicity (given in section 2), and to demonstrate that for gratings with 1D periodicity, it is not necessary to have small period in order to observe the total absorption for shallow grooves. The second aim of the paper is to provide a physical explanation of this phenomenon by comparison with a metamaterial anisotropic layer with equivalent refractive index, given by the homogenisation (quasistatic) limit of the grating when its period tends to zero. To this aim, we discuss in section 3 the reflection properties of a homogeneous but anisotropic layer on a silver substrate, which presents refractive properties, equivalent to the grating in the homogenized limit, when the period becomes much shorter than the wavelength. The analysis is then extended in the complex plane of the propagating constant the PSW, in order to determine its role in the absorption of light by shallow lamellar gratings.

The numerical methods used for modelling of the grating structures are based on the so-called rigorous coupled wave (RCW) method, recently known also under the name of Fourier modal method. The 1D version has been proposed by Peng et al. [15], Krupitsky and Chernov [16], and Moharam and Gaylord [17], and improved through the works of Lalanne and Morris [18] and Granet and Guizal [19]. The 2D method has been developed by Li [20]. Detailed review of the method is available in [21].

2. Light absorption by fine-pitch lamellar gratings with one- or two-dimensional periodicity

The structures under considerations are sketched in Fig. 1, together with some notations and coordinate system. We consider silver lamellar gratings (optical indices given in [22, 23]) with one- or two-dimensional periodicity (Fig. 1(a) and 1(b)), deposited on a silver substrate. The period is d (it is the same in both x - and z - directions for the 2D case), the channel width is c , and its depth is h . The incident vector lies in the xOy plane. We distinguish transverse electric (TE), or transverse magnetic (TM) cases, with electric or magnetic field vector perpendicular to the plane of incidence, and unpolarized light, which is the mean of the two. Figure 1(a) shows the TM polarization with magnetic field \vec{H} perpendicular to the plane of incidence.

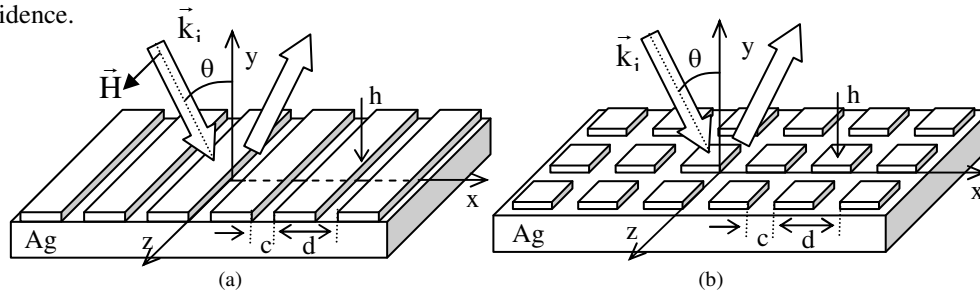


Fig. 1. Sketch of lamellar diffraction gratings, together with the coordinate system and notations: grating with 1D (a) and 2D (b) periodicity.

Figure 2 presents the reflectivity of a 2D structure as a function of the groove width c of the groove depth h with $d = 60$ nm and 120 nm, wavelength $\lambda = 457$ nm, and in normal incidence, with properties independent of the incident polarization. One can observe a relatively broad minimum that appears at very shallow groove depth, smaller than $\lambda/20$, and more than two times shallower than the 1D or 2D gratings representing total absorption due to the excitation of PSW [6, 8]. In addition, the absorption covers a wide interval of incidence angles, as observed in Fig. 3 for the two fundamental polarizations of incident light. The same relatively large absorption domain is observed in the spectral dependence, as shown in Fig. 4. Note the semilogarithmic scale.

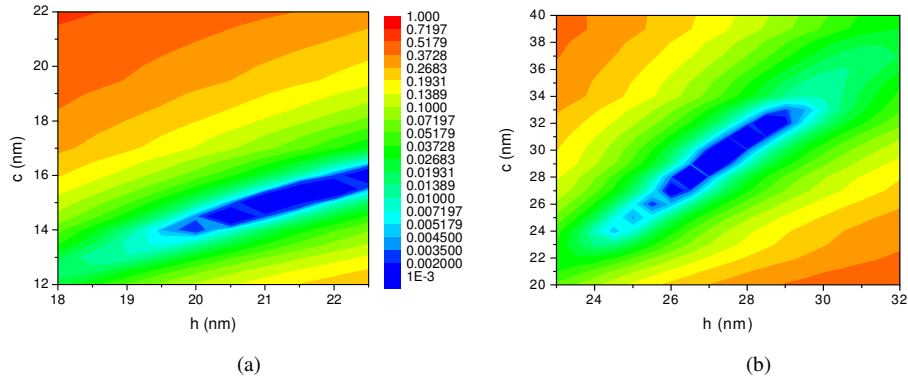


Fig. 2. Reflectivity of the grating sketched in Fig. 1(b) as a function of the groove depth h and the channel c . Period $d = 60$ nm (a), 120 nm (b), wavelength $\lambda = 457$ nm, normal incidence, arbitrary polarization.

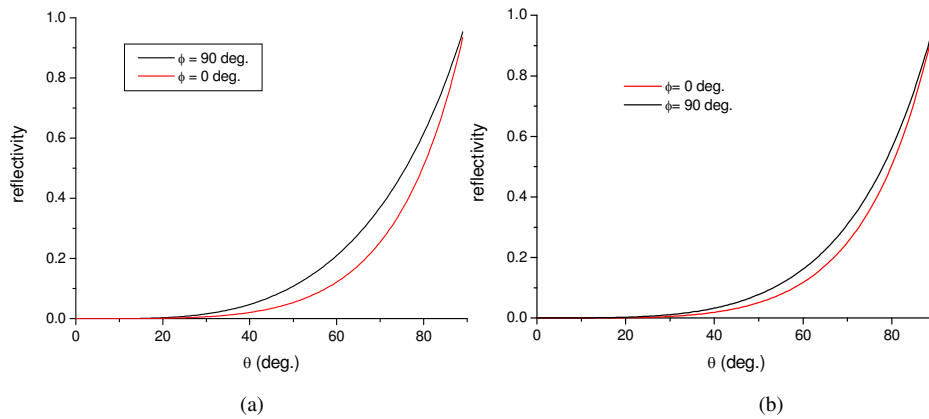


Fig. 3. Angular dependence of the reflectivity of the grating sketched in Fig. 2. Two fundamental polarizations with respect to the plane of incidence, $\lambda = 457$ nm, TE case with the angle between the plane of incidence and the incident electric field vector $\Phi = 90^\circ$, and TM case with $\Phi = 0$. (a) $d = 60$ nm, $c = 15$ nm, and $h = 21.5$ nm, (b) $d = 120$ nm, $c = 30$ nm, and $h = 27.5$ nm.

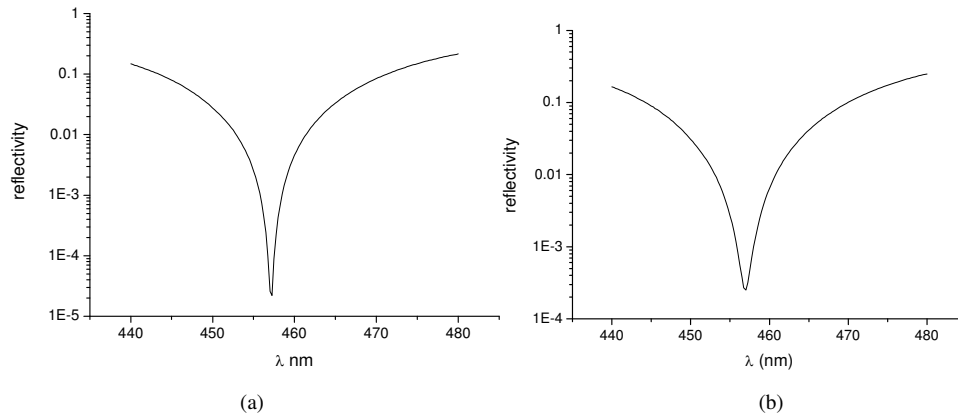


Fig. 4. Spectral dependence of the reflectivity in normal incidence and arbitrary polarization for the grating with 2D periodicity. Same parameters as in Figs. 3(a) and 3(b).

One-dimensional (classical) gratings present similar behavior, as observed in Fig. 5(a) for two different values of c/d . Total absorption appears even for shallower grooves, but only in TM polarization. Moreover, as observed in Fig. 5(b) that gives the angular distribution of the reflectivity with the period varying from 205 nm to 0.01 nm, total light absorption is always present, provided the optimal choice of the groove depth value. Although the last example is quite unrealistic and rises the question of validity of macroscopic refractive index, it represents the homogenized (quasistatic) case, in which one can use the concept of effective medium. The wavelength $\lambda = 457$ nm is more than twice the largest period, so that the gratings support only the specular diffraction order.

The authors of [14] explain the effect thanks to the analysis of the fundamental cavity mode that can propagate inside the groove, and that corresponds to the TEM mode for perfectly conducting walls. However, this explanation cannot hold in the case of $d = 0.6$ nm, when taking into account that the skin depth of silver around 450 nm wavelength is of the order of 10-12 nm. In addition, the concept of TEM modes is questionable for 2D crossed channels.

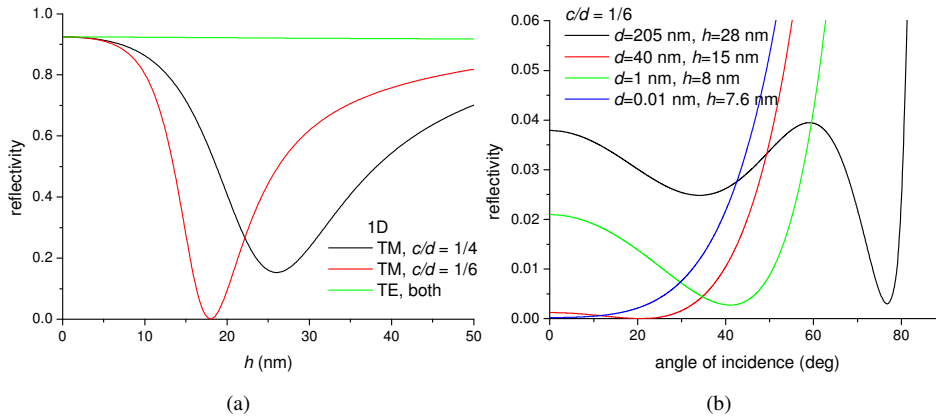


Fig. 5. Reflectivity of a grating with 1D periodicity (as given in Fig. 1(a)). (a) Groove depth dependence with period $d = 60$ nm, wavelength 457 nm, normal incidence. (b) Angular dependence for different periods and groove depth, with $c/d = 1/6$.

3. Reflection properties of the equivalent metamaterial layer

In order to understand why such shallow gratings can totally absorb incident light, we present in Fig. 6 the real part and the imaginary parts of the equivalent relative dielectric permittivity $\bar{\epsilon}$ as a function of c/d and λ . The equivalent layer is anisotropic and its permittivity is calculated as the arithmetic or harmonic mean value of the permittivities of the filling materials, silver ϵ_m and air ϵ_a , in our case. One-dimensional periodic gratings can be characterized by uniaxial medium with ordinary axis along y and z , and extraordinary axis along x , so that [24 - 26]:

$$\bar{\epsilon}_x = \frac{d}{(d-c)/\epsilon_m + c/\epsilon_a} \quad (1)$$

$$\bar{\epsilon}_y = \bar{\epsilon}_z = \frac{(d-c)}{d}\epsilon_m + \frac{c}{d}\epsilon_a \quad (2)$$

3.1. Qualitative analysis in the 2D case

In the case of 2D periodical grating, the ordinary axis is along y , while the symmetry of the structure in x and z directions creates symmetry of the equivalent permittivity [27, 28]:

$$\bar{\epsilon}_x = \bar{\epsilon}_z = \epsilon_a \frac{(1+f)\epsilon_m + (1-f)\epsilon_a}{(1-f)\epsilon_m + (1+f)\epsilon_a}, \quad (3)$$

$$\bar{\epsilon}_y = f\epsilon_m + (1-f)\epsilon_a, \quad (4)$$

where

$$f = \left(1 - \frac{c}{d}\right)^2 \quad (5)$$

is the filling factor. The black line in Fig. 6(a) represents the 0th isovalue line of $\text{Re}(\bar{\epsilon}_x)$, i.e., the transition between dielectric and metallic properties. As can be observed, for very small channel width, the layer behaves like bulk silver. However, as c/d increases, a region appears in the long-wavelength limit that presents resonance of the same type as the plasmon resonance around 325 nm, but of inverted kind – with the increase of the wavelength at a given c/d ratio, the portion of the dielectric in the ‘alloy’ becomes relatively more important and the metamaterial is transformed from a conducting metal to lossy dielectric. Increasing the groove width leads to a blue shift of this metamaterial resonance, so that at 457 nm it can be observed at c/d close to 0.15.

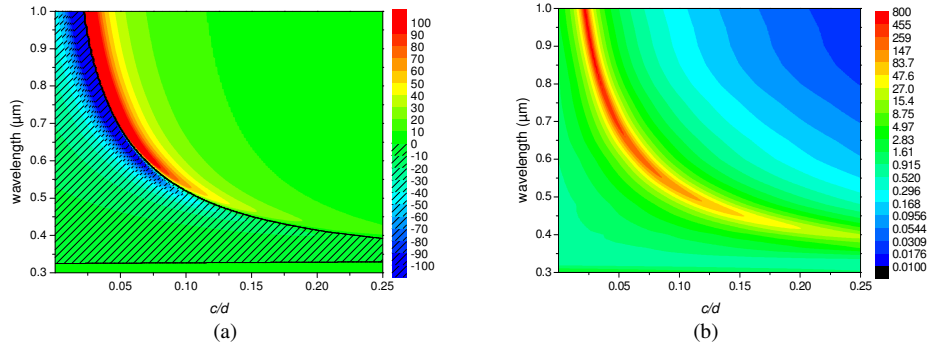


Fig. 6. The effective permittivity along the extraordinary axis as given by Eqs. (3) and (4) as a function of c/d and λ . (a) $\text{Re}(\bar{\epsilon}_x)$, black line for $\text{Re}(\bar{\epsilon}_x)=0$ and the hatched zone for $\text{Re}(\bar{\epsilon}_x) < 0$, (b) $\text{Im}(\bar{\epsilon}_x)$.

The difference between the classical dielectric and the metamaterial ‘alloy’ is that the real part of the equivalent refractive index can become significantly higher than all known dielectrics at this wavelength. For example, with $c/d = 1/6$ at 457 nm, the equivalent refractive index obtained from Eqs. (1) and (3) is respectively equal to $\bar{n}_x = 4.852 + i0.9126$ and $\bar{n}_x = \bar{n}_z = 5.29 + i1.62$. The mean arithmetic refractive index, obtained from Eq. (4) is equal to $\bar{n}_y = 0.127 + 2.04$. Close to normal incidence this index plays no role, as the electric field vector has no y -component. The reflection is then determined by only \bar{n}_x or \bar{n}_z , which both correspond to lossy dielectric, which explains the total absorption for unpolarized light. Figure 7 gives the reflectivity of such anisotropic layer deposited on a silver substrate as a function of the layer thickness; the same dependence is obtained when using isotropic layer with index equal to \bar{n}_x . A minimum of about 4% is observed for very thin layer (thickness 6.2 nm), about 1/70 of the incident wavelength, and the low reflectivity is preserved in a large interval of angle of incidence and wavelength values, as observed in Fig. 8.

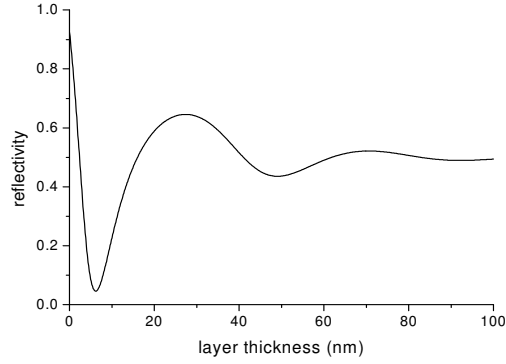


Fig. 7. Reflectivity of a homogenous layer with optical index equal to $5.29 + i 1.62$ on a silver substrate as a function of the layer thickness. Normal incidence with $\lambda = 457$ nm.

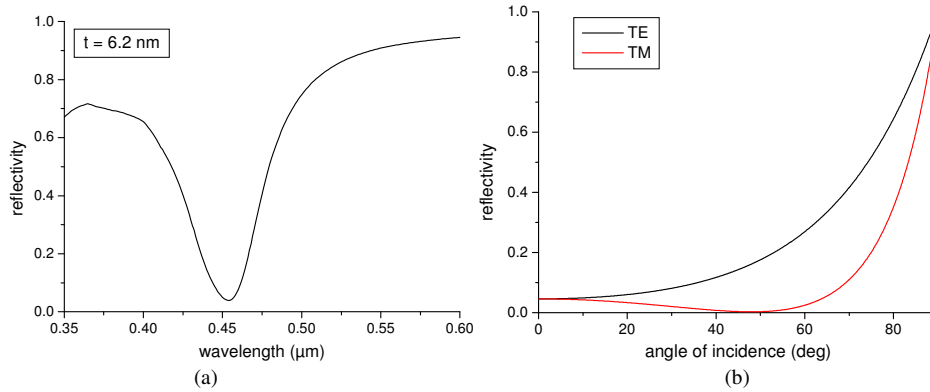


Fig. 8. Reflectivity of an anisotropic homogeneous layer with thickness 6.2 nm deposited on a silver substrate: (a) spectral dependence in normal incidence, both polarizations, (b) angular dependence for $\lambda = 457$ nm, polarizations as indicated in the figure.

This behavior is quite similar to the reflectivity of the 2D grating in Figs. 3 and 4. However, due to convergence problems, we cannot calculate its reflectivity for very small periods in order to quantitatively compare it with the homogenized layer. This comparison can easily be done in the 1D periodical case, and the results are presented in the next subsection. However, simple analysis can explain why quite thin metamaterial layer with equivalent permittivity that presents lossy dielectric and equivalent permeability equal to 1 can strongly absorb incident light. Let us consider a homogeneous layer (numbered as medium 2), deposited on a plane surface (medium 3) and illuminated from the cladding (medium 1). A simple textbook analysis shows that ratio R of the reflected and incident electric field amplitudes in normal incidence contains two contributions, the reflection from the upper surface $R_{\text{refl.}}$ and the interference factor $R_{\text{interf.}}$, due to the multiple reflections inside the layer:

$$R = R_{\text{refl.}} + R_{\text{interf.}} \equiv r_{12} + \frac{t_{12}t_{21}r_{23}}{\exp(-2ik_2h) - r_{21}r_{23}} \quad (6)$$

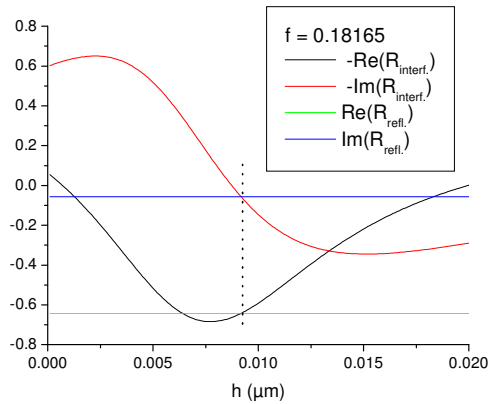


Fig. 9. The reflection and the interference factors (real and imaginary parts) of R as given in Eq. (6), for a homogeneous layer with effective permittivity given by Eq. (3), with $f = 0.18165$, $\lambda = 0.457 \mu\text{m}$, and silver substrate. Permeabilities are equal to 1.

Here r_{ij} and t_{ij} , $i, j = 1 - 3$ represent the Fresnel reflection and transmission coefficients when light passes from medium i into medium j . k_2 is the wavenumber inside the layer. While the first contribution does not depend on the layer thickness, the second one can sometimes fully compensate the first one, which happens with antireflection coatings. A simple program was made to calculate the effective permittivity by using Eq. (3) as a function of f , and R minimized through Eq. (6), for $\lambda = 457 \text{ nm}$ and silver substrate and bumps. An optimal value of $f = 0.18165$ gives total light absorption at $h = 9.2 \text{ nm}$. The corresponding values of the permittivity are $\epsilon_m = -6.4017 + i 0.74292$, $\bar{\epsilon}_x = \bar{\epsilon}_z = 19.033596 + i 7.7116$, and of the indexes: substrate $n_{\text{Ag}} = 0.1466 + i 2.534$, and $\bar{n} = 4.448 + i 0.866$. As can be observed in Fig. 9, for the optimal value of the layer thickness (dotted vertical line), the two terms in Eq. (6) fully compensate each other, i.e., the total light absorption that results can fully be explained by the Fabry-Perot resonance in the equivalent lossy high-index dielectric layer with no magnetic properties.

3.1. Quantitative analysis for the 1D case

The “ordinary” refractive index, determined from Eq. (2) in the 1D case corresponds to a metal, with $\bar{n}_y = \bar{n}_z$ equal to $0.136 + i 2.277$. These indexes play no role in TM polarization close to normal incidence, when the only non-zero component of the electric field is E_x . On the contrary, in TE polarization close to normal incidence, the only component of the electric field is along the z -axis, the system reflects like metal, thus the difference between the two fundamental polarizations in Fig. 5. The reflection properties of such anisotropic but homogeneous layer (it can be taken isotropic in normal incidence), deposited over a plane silver surface are the same as for a very fine-pitch lamellar grating, as observed in the layer depth h dependence given in Fig. 10(a). The curve for the plane homogenized layer can easily be obtained by using Airy coefficients (or even Fresnel coefficients). A sharp minimum occurs at $h = 7.6 \text{ nm}$, with a quasiperiodical behavior due to Fabry-Perot effect as a function of h with a period of about 47 nm , equal to $\lambda / (2 \text{Re} \bar{n}_x)$. The reflectivity of this layer coincides with the reflectivity of 1D periodical grating with very small pitch, when $\lambda/d > 100$. This limit ratio for the homogenisation of the structure seems very high, but in fact, due to the high effective refractive index (of the order of 5), the homogenized limit ratio between the wavelength *inside* the medium and the period becomes of the order of 20.

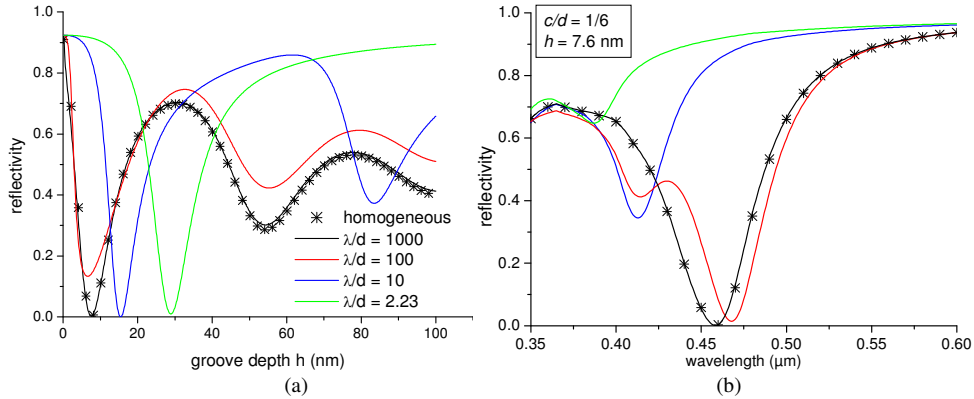


Fig. 10. Reflectivity as a function of the groove depth (a) in normal incidence (TM polarization) for a 1D grating having different λ/d ratio, compared with the reflectivity of a plane homogeneous layer (asterisks) with indexes given in the text. $\lambda = 457$ nm, $c/d = 1/6$. (b) spectral dependence for the same λ/d ratios with $h = 7.6$ nm

The comparison between the spectral dependences of the homogeneous layer and very fine pitch gratings is made in Fig. 10(b) and one can observe identical response in the quasistatic limit. With the increase of the period towards more realistic values, the behavior is quite similar until the homogenisation holds. For larger periods ($\lambda/d = 10$ and 2.23), one observes similar minima and maxima, but with quasiperiod that grows with the grating period. This can be understood in terms of effective index, which diminishes when we exit the quasistatic limit, as seen in Fig. 6. In addition, this explains also the necessity to increase the groove depth in order to obtain (almost) total absorption when the period is larger (see again Fig. 7).

4. PSW cut-off by the metamaterial

As already observed in Fig. 6, for values of c/d larger than 0.15 and $\lambda > 450$ nm, the metamaterial has no plasmonic resonance near normal incidence in TM polarization for the 1D case and in both polarizations for the 2D periodicity. The natural question that rises is whether this is valid out of normal incidence, where the ordinary part of the refractive index has metallic values. In order to find a response, we carried out a search for poles $\alpha_p = k_x/k_0$ of the scattering matrix in the complex α_0 -plane, poles which represent electromagnetic resonances, and, in particular, surface or guided waves that can propagate along the interfaces or guided inside the layer. Due to the absorption losses in both the silver substrate and the metamaterial layer (or the grating, when not in the quasistatic limit), the poles corresponding to the propagation constant of the system modes are complex. There are no radiation losses due to diffraction by the grating in air, because the period is sufficiently small. Let us remind that when α_0 is real and lying between -1 and 1 , $\alpha_0 = \sin \theta$.

We start with $h = 0$ and the only pole that exists corresponds to the PSW that propagates along silver-air interface and its propagating constant is equal to

$$\alpha_p(h = 0) = \pm \sqrt{\epsilon_m \epsilon_a / (\epsilon_m + \epsilon_a)}, \quad (7)$$

the sign minus standing to a PSW propagating in the opposite direction. In the case of a grating, this pole is multiplied by the grating period.

Let us consider the PSW that moves in positive x -direction. When the groove depth starts growing, the losses increase due to the presence of the grating, so that the imaginary part of the poles start to grow, the propagation of the PSW becomes more perturbed, its speed decreases and the real part of the propagation constant also increases, a well known behavior (see for example ref. [29]). What is amazing in our case (both for very small or larger periods) is that very rapidly (for quite small values of h), the trajectory turns in direction of smaller

$\text{Re}(\alpha_p)$, as observed in Fig. 11(a). Further increase of h leads to a rapid decrease of $\text{Re}(\alpha_p)$ below the line $\text{Re}(\alpha_0) = 1$ and the pole is transformed into a Fabry-Perot resonance with high losses. For larger groove depths, the losses start to decrease, and at a given groove depth the trajectory crosses the cut in the complex plane introduced due to the ambiguity of the sign of the square root in Eq. (7) [29].

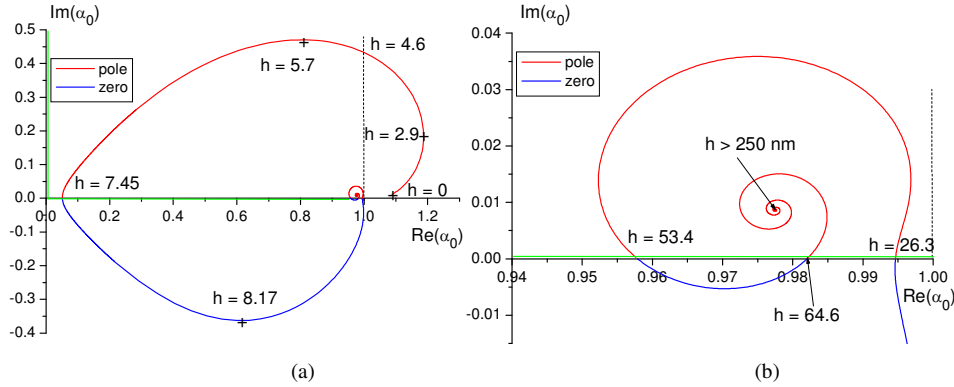


Fig. 11. Trajectory of the pole of the scattering matrix, above the cut in the complex plane presented by a green line, or the corresponding zero of the reflection order below the cut, as a function of the groove depth (given in nm) for a homogeneous anisotropic layer obtained by a 1D periodic grating with $c/d = 1/6$ and $\lambda = 456$ nm. (a) the entire trajectory, (b) zoom close to $\alpha_0 = 1$.

This cut (the green lines in Fig. 11(a)) starts from the branching point at $\alpha_0 = 1$, goes along the real axis down to the origin and then climbs along the imaginary axis, because the resonance that has a positive real part must have also a positive imaginary part in order to stay bounded. When crossing this cut, the pole is transformed into a zero of the reflected order, so that one obtains an absorption of the incident light without resonance. An unexperienced reader can easily understand this transfer from pole (surface plasmon) of the scattering matrix into a zero (Brewster effect) for a single interface between two homogeneous media in TM polarization. The elements of the scattering matrix are the four Fresnel reflection and transmission coefficients, and they all have common denominator, which can lead to a pole, when singular, responsible for the appearance of PSW. In particular, the reflection Fresnel coefficient:

$$r_{12} = \frac{\beta_1 / \varepsilon_1 - \beta_2 / \varepsilon_2}{\beta_1 / \varepsilon_1 + \beta_2 / \varepsilon_2}, \quad (8)$$

with $\beta_j = \sqrt{\varepsilon_j + \alpha_0^2}$, $j = 1, 2$. When α_0 is complex, the choice of the sign of the square root in $\beta_{1,2}$ becomes ambiguous that is solved by introducing cuts in the complex plane, cuts different for each media, as their branching points start at $\beta_j = 0$. As a consequence, when the trajectory of the pole crosses the cut of β_1 , its sign changes, which leads to a permutation of the nominator and denominator of r_{12} in Eq. (8). The result is that the pole (zero of denominator) becomes a zero of the reflection coefficient, i.e., Brewster phenomenon.

When the resulting zero of the reflected wave is real, the absorption becomes total, as it happens for $h = 7.45$ nm for $\lambda/d > 100$. For larger and more realistic periods, the trajectory of the pole (and the zero) differs, so that the crossing of the real axis leading to a total absorption happens for different (and usually larger) groove depth values.

Further increase of the groove depth leads to a new swing of the trajectory of the zero in the lower semi-plane of complex α_0 , as seen in Fig. 11(b). A new approach to the real α_0 -axis, this time close to grazing incidence means new case of total absorption. Quite interesting is

the spiral convergence of the trajectory of the pole-zero, when the groove depth is further increased to infinity. The limit is easily reached for not so great groove depths, h close to 250 nm is sufficient (see further Fig. 12(a)), because of the relatively high imaginary part of the effective refractive index (0.91 in our case), so that the system behaves like as if having infinitely deep grooves. In terms of equivalent metamaterial layer, this means that we can consider it semi-infinite, so that the only resonance is the pole approximately given by Eq. (7) replacing ϵ_a with $\bar{\epsilon}_x$. In fact, Eq. (7) stays both for plasmon surface wave (the zero of the denominator of the Fresnel reflection coefficient, or for a zero of the nominator of the reflection Fresnel coefficient. The exact Brewster law for the anisotropic layer is more complex to determine than Eq. (7), because of the different effective index in vertical direction. Simple considerations using the boundary conditions at the metamaterial-air interface give the formula:

$$\alpha_{p,\text{aniso}} = \epsilon_1 \bar{\epsilon}_y \frac{\epsilon_1 - \bar{\epsilon}_x}{\epsilon_1^2 - \bar{\epsilon}_x \bar{\epsilon}_y} \quad (9)$$

The numerical values obtained by using Eqs. (7) and (9) are quite similar, $0.98177 + i 0.00716$ and $0.9775 + i 0.00867$, respectively. The latter value is the exact limit of the spiral in Fig. 12(b), and gives an almost real Brewster angle close to grazing incidence, which is not surprising, since the equivalent layer is dielectric (in x-direction) with high equivalent index, real part almost 5, so that the Brewster angle is approximately equal to $\arctg(5) \approx 78.5^\circ$. The localization of the pole/zero close to grazing incidence for large interval of groove depths leads to a strong light absorption around 80° incidence when $h > 50$ nm, as observed in Fig. 12(a).

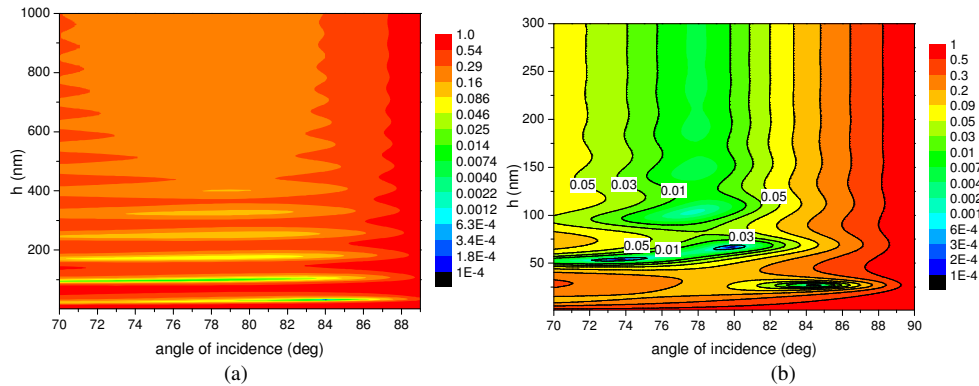


Fig. 12. Reflectivity of a homogeneous anisotropic layer (a) and of 1D grating ($d = 60$ nm, $c = 10$ nm) as a function of the angle of incidence and groove depth. Wavelength 456 nm, TM polarization.

When the period is held more realistic, then trajectory of the pole/zero changes, but stays similar to the one presented in Fig. 11, which leads to low reflectivity in grazing incidence, as observed in Fig. 12(b). The saturation groove depth is greater than in Fig. 4, because the effective refractive index is smaller in this case, as observed in Fig. 11.

We have demonstrated that in the homogenized case the full absorption is not due to surface plasmons but to Fabry-Perot resonance or Brewster effect, depending on the anisotropic layer thickness. However, a question stays open whether the surface plasmon can propagate in similar conditions, but when the groove period is much greater than the homogenized limit. We have observed in Fig. 10 that, for example with $d = 60$ nm, the absorption is still achieved but for higher values of groove depth (typically $h = 16,5$ nm). Figure 13 shows the trajectory of the pole of the scattering matrix in the complex plane in the case of a 1D grating with $d = 60$ nm. As compared with Fig. 11(a), the behavior is the same, i.e. the propagation of the plasmon surface wave is cut for groove depths larger than few nanometers. The trajectory

crosses the real axis when $h = 16.5$ nm, which leads to a full absorption, in the same manner as in the homogenized case. However, the study of the light intensity in the neighborhood of the corrugated layer shows a strong enhancement on the groove top, which can be interpreted as excitation of localized plasmons (Fig. 14). The amplitude of these resonances diminish when the period is reduced, and they are transformed into Fabry-Perot resonance in the quasi-static limit ($d < \lambda/100$).

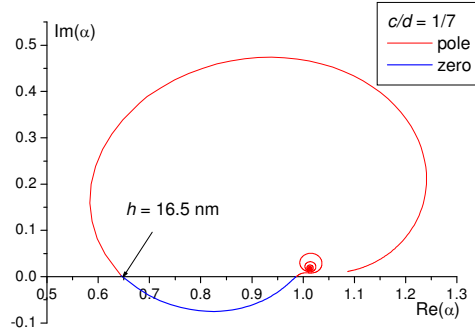


Fig. 13. Trajectory of the pole of the scattering matrix, or the corresponding zero of the reflection order below the cut, as a function of the groove depth (given in nm) for a 1D periodic grating with $c/d = 1/7$ and $\lambda = 456$ nm.

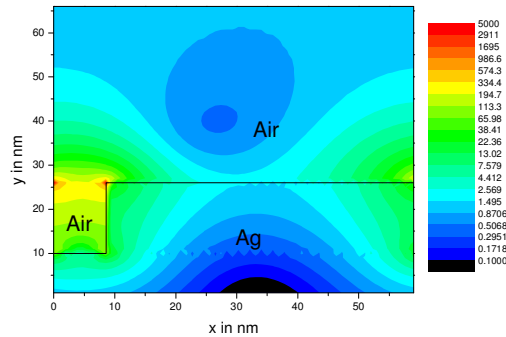


Fig. 14. Light intensity on one period of a 1D grating when illuminated in oblique incidence, $\theta = \sin^{-1}(0.65)$ (see Fig. 13) in TM polarization, with $d = 60$ nm, $h = 16$ nm, $c/d = 1/7$ and $\lambda = 456$ nm..

6. Conclusion

We have shown that the total absorption of very shallow gratings could be obtained and understood thanks to their metamaterial behavior for small periods. Metamaterial denomination is fully justified by the fact that we show that the homogenized material exhibits higher optical index than any known dielectric (in this range of wavelength). The trajectory of the pole in the quasi-static limit has shown that the full absorption is due to Fabry-Perot resonance or Brewster effect (depending on the thickness of the anisotropic layer). As a consequence, the full absorption can be explained without the role of plasmons, and the metamaterial exhibits a total aplasmonic behaviour. Outside the quasi-static limit, the corrugated layers exhibits a strong metallic behaviour, with a strong light intensity enhancement due to localized plasmons, but optical properties are similar to the one presented in the homogeneization case. The difference lies in the depth of the absorbing layer, which is higher (16 nm in the case of silver at 456 nm for $d=60$ nm) outside the homogeneization limit.